

# Synergism Effect Between Modified Carbon Black and Organic Ultraviolet Absorber in Polymer Matrix for Ultraviolet Protection

Q. F. Shi,<sup>1</sup> J. Y. Gao,<sup>2</sup> D. D. Zhao,<sup>1</sup> S. A. Xu<sup>1</sup>

<sup>1</sup>Key Laboratory for Preparation and Application of Ultrafine Materials of Ministry of Education, School of Material Science and Engineering, East China University of Science and Technology, Shanghai 200237, China

<sup>2</sup>School of Chemistry and Molecular Engineering, East China University of Science and Technology, Shanghai 200237, China

Received 11 June 2008; accepted 8 November 2009

DOI 10.1002/app.31775

Published online 20 January 2010 in Wiley InterScience (www.interscience.wiley.com).

**ABSTRACT:** Modified carbon black (MCB) was obtained by oxidization and hydroxymethylation reactions with conductive carbon black (CB); in the MCB, some hydroxyl groups were introduced on the surface of the CB particles. CB, MCB, and a kind of organic ultraviolet absorber (UA) were used as UV antidotes, and binary composites and ternary composites were prepared by solvent casting with polystyrene, styrene-butadiene-styrene triblock copolymer, and poly(methyl methacrylate) as the matrix, respectively. In the binary composites, only one kind of UV antidote was used, whereas in the ternary composites, the organic and inorganic UAs were combined. The ultraviolet-visible absorption spectra of the composites were

investigated extensively, and it was found that no synergism occurred when CB was combined with the organic absorber; on the other hand, an obvious synergism effect emerged when MCB was combined with the organic absorber in the same matrix, which was attributed to the formation of hydrogen bonds between MCB and UA. The interaction between MCB and UA was studied by Fourier transform infrared spectroscopy, differential scanning calorimetry, and transmission electron microscopy. © 2010 Wiley Periodicals, Inc. *J Appl Polym Sci* 116: 2566–2572, 2010

**Key words:** blends; elastomers; films; UV-vis spectroscopy

## INTRODUCTION

The UV protection of organic or polymer materials against photodamage is of high practical interest. This protection can be realized by the addition of organic or inorganic ultraviolet absorbers (UAs). Ideal UV-protection materials should exhibit strong absorptions in the UV range (200–400 nm) and be transparent in all visible light (>400 nm). UAs are also usually used in cosmetics to prevent sunburns and skin cancer.<sup>1,2</sup>

The organic UAs used frequently contain azimino-benzene derivatives and benzophenone derivatives in the commercial field, whereas the titanium dioxide, silicon dioxide, and carbon black (CB) are usually used as inorganic UAs for material protection. Although organic and inorganic UAs can both be used to shield UV irradiation, their mechanisms are completely different. Inorganic UAs screen UV light

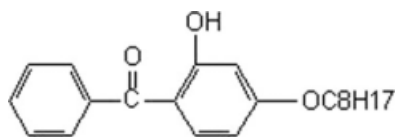
mainly by reflection and refraction, whereas organic UAs protect materials through conversion of light energy into heat by a tautomerization reaction or by their own decomposition.<sup>3</sup>

Unfortunately, although organic or inorganic UAs used alone cannot provide desired protective functions, a great improvement in performance can be achieved by the combination of two types of UAs. Mahltig et al.<sup>4</sup> combined TiO<sub>2</sub> with organic UAs and prepared composites with perfect UV absorption.

It is well known that CB is widely used in many fields. Researchers have characterized its properties by many techniques, including high-resolution transmission electron microscopy (TEM), <sup>13</sup>C-NMR, and ultraviolet-visible (UV-vis) spectroscopy.<sup>5,6</sup> Jager et al.<sup>5</sup> investigated the correlation between the internal structure and spectral behavior of CB. In their research, the internal structure of primary CB particles was explored by high-resolution TEM, electron energy loss spectroscopy, <sup>13</sup>C-NMR, and Raman spectroscopy. Michel et al.<sup>6</sup> proposed a simple model for the optical properties of CB particles, in which the particles were considered to be a mixture of two materials: a graphitic and an amorphous material. Moreover, CB has been used as an established light-stabilizing additive in polyolefin (and other

Correspondence to: S. A. Xu (saxu@ecust.edu.cn).

Contract grant sponsor: Natural Science Foundation of Shanghai; contract grant number: 02 ZE 14023.



**Scheme 1** Chemical structure of UV531 (UA).

polymers) for many years, and it has the potential to function as a simple physical screen, UA, radical trap, and terminator of free-radical chains.<sup>7</sup>

Pena et al.<sup>8</sup> studied the interactions between two commercial hindered piperidine compounds, three commercial antioxidants, a secondary antioxidant, and two types of furnace CBs in the photooxidation of low-density polyethylene, and they found that the interactions were different, being antagonistic or synergistic depending on the chemical structure of the organic compounds and the combinations of these additives. Moreover, they concluded that the nature of CB played an important role in the control of its performance as a stabilizing agent alone and in its interactions with light stabilizers and antioxidants. Liu and Horrocks<sup>7,9</sup> also studied the combined effects of selected CB pigments and hindered light stabilizers on the UV stabilities of linear low-density polyethylene films under two kinds of UV radiation sources, and they found that presence of each CB resulted in a significant improvement in UV stabilization compared to clear films, especially for those with small particle sizes; as expected, the photostabilizing efficiency of CB was based on both the physical surface-area-dependent UV absorption and the photochemical activity.

Although related literature has reported the protection of CB to UV light and interactions with organic UAs, CB was used as received without any modification. CB is composed of primary particles with diameters of 10–75 nm, which are fused into aggregates ranging from 50 to 500 nm in size. Beyond the basic structures of primary particles and aggregates, CB can easily form agglomerates held together by Van der Waals forces,<sup>10</sup> which confines its application in many fields. To improve the dispersion of CB in either the polymer matrix or the solvent, a great many efforts have been devoted to the surface modification of CB.<sup>11–15</sup> However, little attention was paid to the UV absorption properties of the modified carbon black (MCB) and its interactions with the organic UAs. In this study, CB was modified by oxidation and hydroxymethylation reactions, and the UV absorption behaviors of MCB were studied in different polymer matrices. To improve the UV-resistant ability of the composites, MCB was combined with a kind of organic UA, and the interaction and the synergism between MCB and the organic UA were intensively investigated.

## EXPERIMENTAL

### Materials

The organic UA UV531 was purchased from Nanjing Hua Lim Co., Ltd. (Nanjing, China), and it was directly used without further purification. The UA was a derivative based on benzophenone, and its chemical structure is shown in Scheme 1. CB (N220) was supplied by Cabot, Inc. (Shanghai, China). Styrene–butadiene–styrene triblock copolymer (SBS; Hunan YueYang Petrochemical Co., Ltd., YH-792, Hunan, China), polystyrene (PS; Ningbo FuTian Co., Ltd, PS-80, Ningbo, China), and poly(methyl methacrylate) (PMMA; LG Co., Ltd, PMMA-850, Seoul, Korea) were used as the polymer matrices for the preparation of the composite films.

### Preparation of MCB

Original CB (N220, 10 g) was added to 100 mL of nitric acid at 90°C, and this solution was stirred for 2 h. The product [oxidized carbon black (OCB)] was filtered and washed with distilled water until the eluting water revealed a neutral pH; then, the filtrate was dried in a vacuum oven at 50°C for 24 h. Thereafter, 5 g of OCB was mixed with 50 mL of formaldehyde and 5 mL of NaOH (20 wt %) in a flask; the mixture was heated to 50°C in a nitrogen atmosphere and stirred for 5 h. The product was purified according to the same procedure used for OCB, and MCB was obtained.

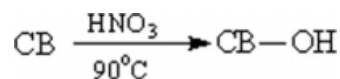
The main chemical reactions occurring in these processes are shown schematically in Schemes 2 and 3.

### Preparation of the composite films

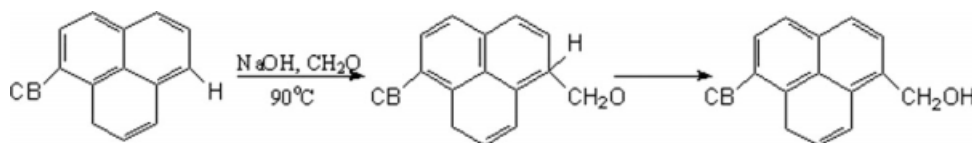
The polymer (SBS, PS, or PMMA) and the organic UA were dissolved in toluene under stirring, and then, CB or MCB was dispersed into the solution under an ultrasonic frequency. The solution was coated on the glass slide, and the composite film was formed after the solvent evaporated. The thickness of the films was about 20 μm. Three kinds of films were prepared and studied, including pure polymer films, binary composite films in which only a single UA was added, and ternary composite films containing both organic and inorganic UAs.

### Characterization

The transmission spectra of the composite films on the glass slides were measured with a UV–vis spectrometer TU-1810 PC (Beijing Purkinje General Instrument Co., Ltd., Beijing, China) in the range



**Scheme 2** Oxidization of CB.



Scheme 3 Hydroxylation of OCB.

200–600 nm. The measurement of IR spectroscopy was conducted with a Nicolet (Madison, WI) AVATAR 360 Fourier transform infrared (FTIR) spectrometer.

Differential scanning calorimetry (DSC) measurements were performed on a 200 PC DSC calorimeter (Netzsch Instruments, Bayem, Germany) under a nitrogen atmosphere (20 mL/min). The sample was heated from  $-140$  to  $60^\circ\text{C}$  at a heating rate of  $10^\circ\text{C}/\text{min}$ .

The organic UA was dissolved in the dilute solution of SBS in toluene; then, CB or MCB was dispersed in the solution under an ultrasonic frequency. The dispersion was coated onto copper mesh to form a film for evaluation by TEM (Hitachi-300 transmission electron microscope, 60 kV, Tokyo, Japan).

## RESULTS AND DISCUSSION

### UV-vis spectra of the binary composite films

For convenience, the effective UV absorption range was defined as the area in which the transmittance ( $T$ ) was less than 10%, and the largest wavelength in the effective UV absorption range was designated as  $\lambda_{\text{max}}^E$ .

Figure 1 shows the UV-vis spectra of SBS and its composite with the organic UA; the content of UA was 2 wt % respective to the matrix. As shown, the effective UV absorption range of SBS was broadened somewhat after the addition of UA. However, the effective UV absorption range was almost the same, which meant that the UV resistance of the polymer

composite containing UA was not greatly improved compared to the pure polymer. A similar phenomenon was also observed in the PS and PMMA matrices, as shown in Figures 2 and 3, respectively.

Some researchers<sup>8,16</sup> reported that a good UV protecting function could be achieved by a combination of organic and inorganic UAs, and CB was frequently used in their research. To broaden the screening range to UV radiation, CB and MCB were combined with an organic UA. MCB was prepared by oxidization and hydroxymethylation reactions. The IR spectra of CB, OCB, and MCB are shown in Figure 4. The original CB did not exhibit the peaks corresponding to hydroxyl and carbonyl groups. After oxidization, OCB exhibited a peak at  $3428\text{ cm}^{-1}$  corresponding to the hydroxyl group and a very weak peak at  $1728\text{ cm}^{-1}$  corresponding to the carbonyl group; this indicated that the hydroxyl groups and minor carbonyl groups were introduced onto the surface of CB. The peaks at  $3420$  and  $1720\text{ cm}^{-1}$  in MCB corresponded to the vibrations of the hydroxyl and carbonyl groups, whereas the peaks at  $2925$  and  $2850\text{ cm}^{-1}$  corresponded to the stretching vibrations of methylene at the hydroxymethyl group; this implied that the hydroxymethyl groups were introduced after hydroxymethylation. Also, the original CB, OCB, and MCB all exhibited a peak around  $1600\text{ cm}^{-1}$  corresponding to the C=C group.

The UV-vis spectra of the polymer composites with CB or MCB on the glass slide are given in Figure 5(a–c). As shown in these figures, there were no

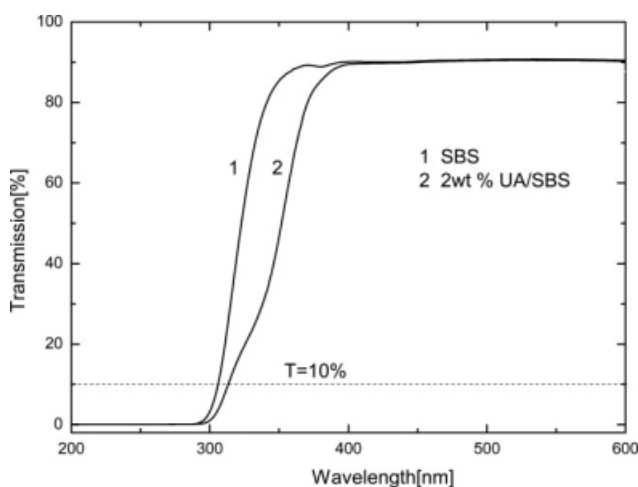


Figure 1 UV-vis spectra of the SBS and UA/SBS composite (2 wt % UA).

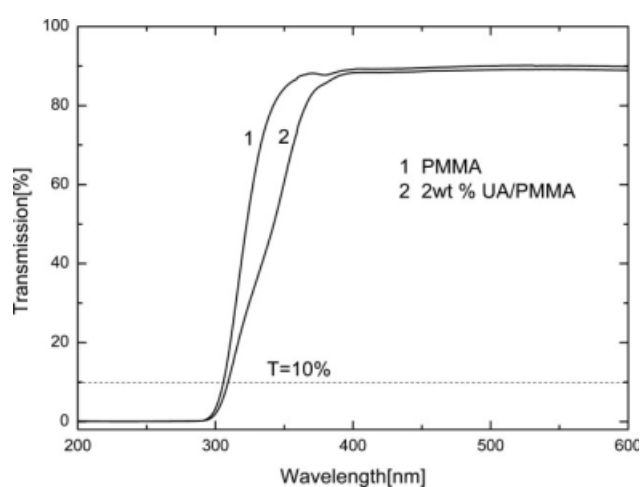
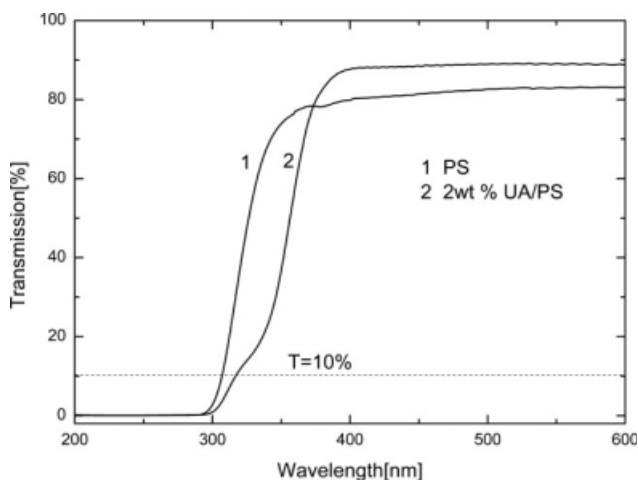


Figure 2 UV-vis spectra of the PMMA and UA/PMMA composite (2 wt % UA).



**Figure 3** UV-vis spectra of the PS and UA/PS composite (2 wt % UA).

great differences in the UV-vis spectra between the CB composites and MCB composites on the glass slide for the same matrix, and the absorption behaviors of the CB or MCB composites were similar to that of the matrix. This means that the UV protection efficiency of the polymers was not improved by the addition of CB or MCB alone.

#### UV-vis spectra of the ternary composite films

To decrease the transmission of coatings over the UV range (200–400 nm), the organic UA was embedded into the CB/polymer or MCB/polymer composite films. The UV-vis spectra of the CB and MCB composites containing UA are shown in Figure 6; in these composites, the content of UA was fixed at 2 wt %, and the weight fraction of CB or MCB was 0.2 wt %. For the UA-embedded MCB/SBS films shown in Figure 6, the transmission of UV light decreased

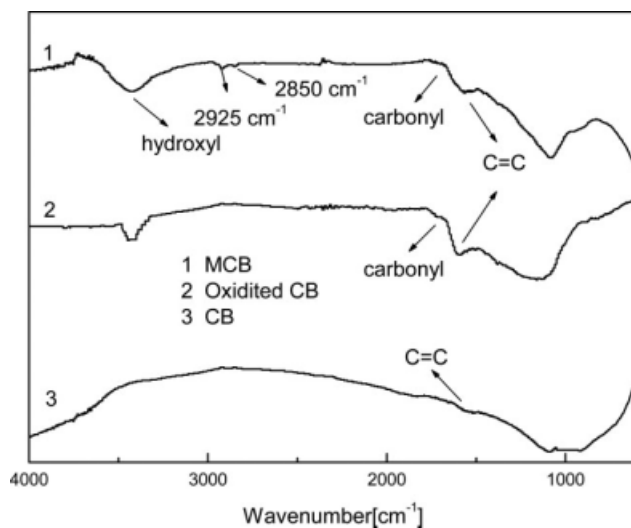


**Figure 4** FTIR spectroscopy of CB, OCB, and MCB.

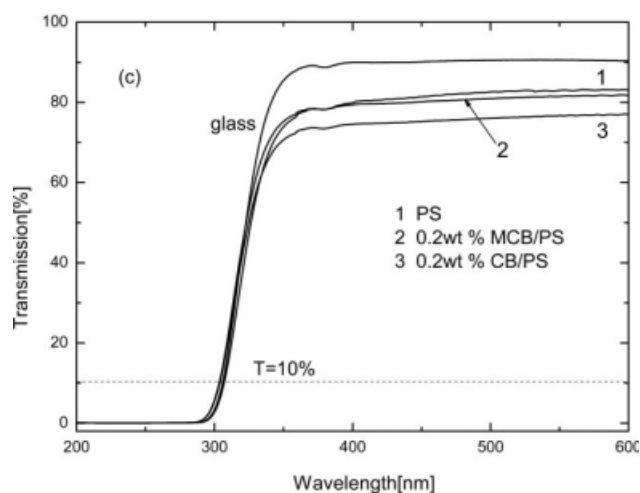
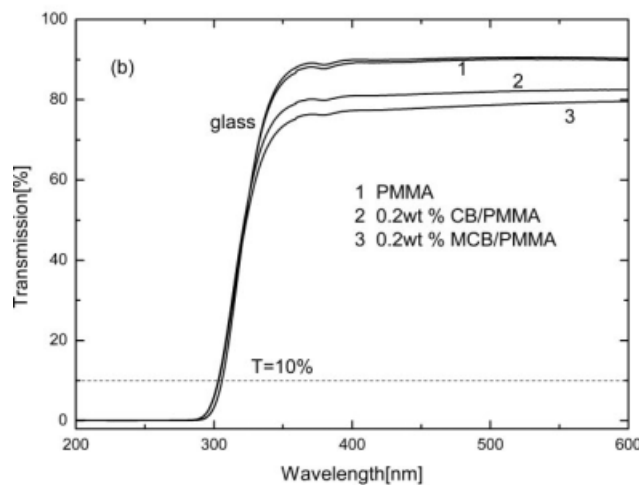
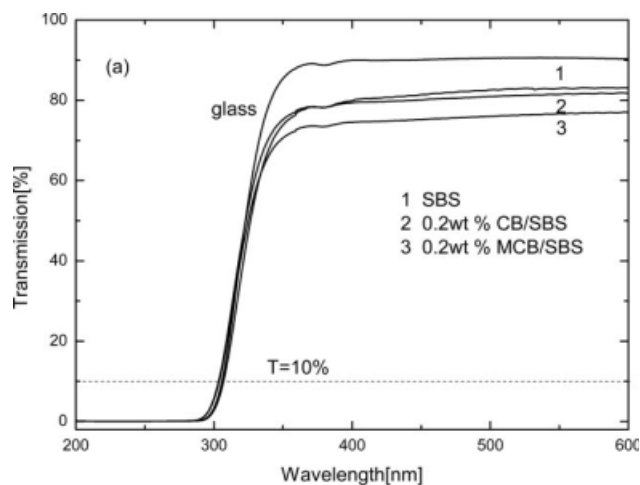


**Figure 5** UV-vis spectra of the (a) CB/SBS and MCB/SBS, (b) CB/PMMA and MCB/PMMA, and (c) CB/PS and MCB/PS composites containing 0.2 wt % CB or MCB.

obviously, and its effective UV absorption range also broadened.  $\lambda_{\text{max}}^E$  extended from 313 to 338 nm; this implied that a redshift occurred in the ternary UA/MCB/SBS composite compared to the binary UA/SBS composites (see Figs. 1 and 6). However, the UA/CB/SBS film did not show a redshift.



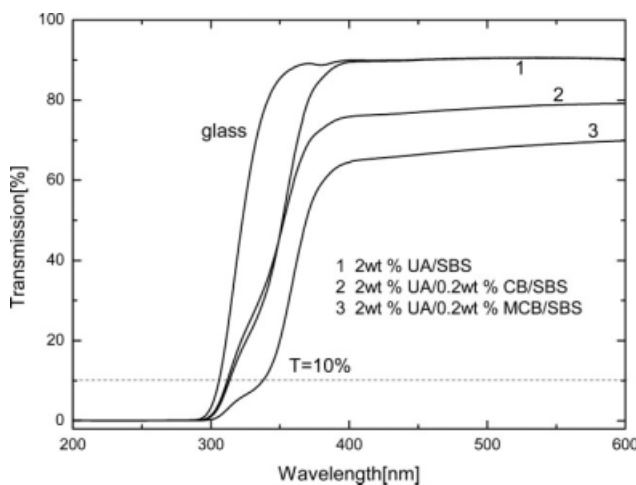


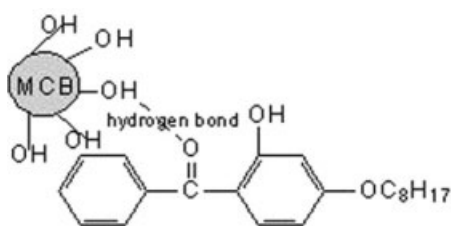
**Figure 6** UV-vis spectra of UA/CB/SBS and UA/MCB/SBS.

The phenomenon of the redshift was also observed in the PS and PMMA composites when MCB was combined with UA, although the redshift was very slight for the PMMA matrix. The UV-vis spectra of the PS and PMMA composites are shown in Figure 7(a,b).

#### Interaction between MCB and UA

In the same matrix, whether MCB or UA was used alone, the synergism effect was not obvious, whereas when MCB and UA were combined, a distinct synergism occurred, which suggested that the interaction between MCB and UA may play an important role in the UV-vis spectra of the composites. To explain the synergism and the redshift phenomenon, the interaction between MCB and UA was studied by FTIR spectroscopy, DSC, and TEM.

After CB was modified by the oxidation and hydroxymethylation reactions, the hydroxyl groups were introduced onto the surface of CB. As shown in Scheme 4, the two benzene rings and the carbonyl group between them in the UA molecule produced a strong conjugation effect, which resulted in the enhancement of the electronegativity of the carbonyl group; therefore, hydrogen bonds might have formed between the carbonyl and hydroxyl groups on the surface of MCB.



**Scheme 4** Formation of hydrogen bonding between MCB and UA.

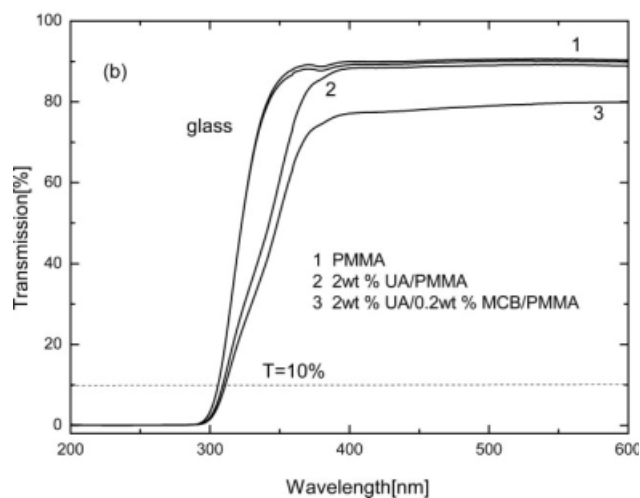
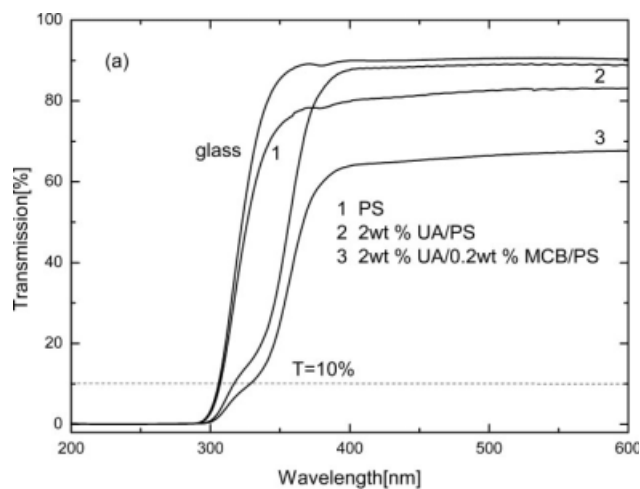


**Figure 7** UV-vis spectra of (a) UA/PS and UA/MCB/PS (2 wt % UA and 0.2 wt % MCB) and (b) UA/PMMA and UA/MCB/PMMA (2 wt % UA and 0.2 wt % MCB).

Also, the phenolic hydroxy in the UA molecule may have formed hydrogen bonds with the hydroxy on the MCB surface.

Figure 8 shows the FTIR spectra of UA, MCB, and their mixture (UA/MCB = 10/1). For comparison, the FTIR characteristic absorption wave numbers of MCB, UA, and their mixture are given in Table I. Because of the strong conjugation effect, the peak of UA corresponding to the stretching vibration of the carbonyl group moved to  $1630\text{ cm}^{-1}$ , and the peak of the stretching vibration of the carbonyl group in

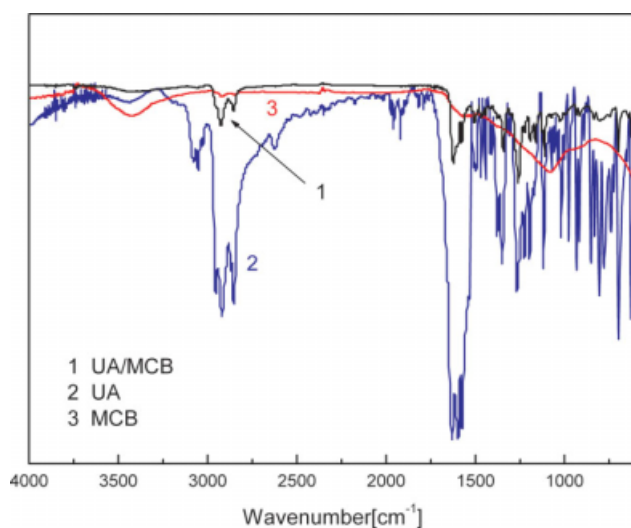


**Figure 8** FTIR spectra of UA, MCB, and their mixture. [Color figure can be viewed in the online issue, which is available at [www.interscience.wiley.com](http://www.interscience.wiley.com).]

the UA/MCB mixture appeared at  $1620\text{ cm}^{-1}$ ; this was a shift of nearly  $10\text{ cm}^{-1}$  toward a lower frequency. The shift of the peak for the carbonyl group in the mixture was attributed to the formation of the hydrogen bond. In Table I, the peaks at  $3420$ ,  $3443$ , and  $3413\text{ cm}^{-1}$  corresponded to the vibrations of the hydroxyl groups in MCB, UA, and their mixture, respectively; the peak of the hydroxyl group in UA/MCB moved toward a lower frequency compared with MCB and UA because of the formation of hydrogen bonds between MCB and UA. The shift of the vibration frequency of the hydroxyl group resulting from the formation of hydrogen bonds has also been reported and studied by others.<sup>17,18</sup>

Figure 9 shows the DSC curves of SBS and its composites, and the glass-transition temperatures of the PB block in SBS and its composites are listed in Table II. For the UA/SBS composite, the decrease in the glass-transition temperature was attributed to the plasticization of UA molecules, whereas for the MCB/SBS composite, the decrease in the glass-transition temperature may have resulted from an increase in the free volume of the composite because of the existence of MCB, which was also studied by other researchers at an earlier time.<sup>19</sup> In the composite UA/MCB/SBS, the glass-transition temperature

**TABLE I**  
FTIR Characteristic Absorption Values of MCB, UA, and Their Mixture

	UA		
	MCB	UA	UA/MCB
Carbonyl group ( $\text{cm}^{-1}$ )	—	1630	1620
Hydroxyl group ( $\text{cm}^{-1}$ )	3420	3443	3413

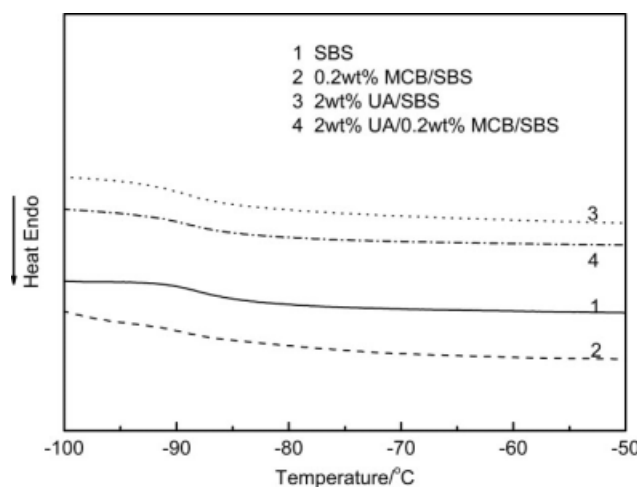


**Figure 9** DSC curves of SBS and its composites.

corresponding to the PB block in SBS of the composite was  $-88.5^\circ\text{C}$ , which was higher than that of UA/SBS composite. This was because some UA molecules dispersed in the matrix migrated to the surface of MCB because of the formation of hydrogen bonds between UA and MCB, which weakened the plasticizing effect of the UA molecules.

Figure 10 shows the TEM micrographs of the UA/MCB/SBS and UA/CB/SBS composites. The average size of the agglomerates of MCB was smaller than that of the unmodified CB; this indicated that the bigger agglomerates of CB were broken into smaller ones after chemical modification. The hydroxyl and hydroxymethyl groups introduced on the surface of CB increased the gap between CB primary particles, and the hydrogen bonds formed between MCB and UA extended the gap further, which made the aggregation of the primary CB particles loose. Therefore, the primary CB particles in the UA/MCB/SBS composite could be clearly identified. Moreover, a core-shell structure of MCB was observed in the UA/MCB/SBS composite [shown as arrows in Fig. 10(b)] because the interval distance between the primary CB particles increased; this was regarded as more evidence for the formation of hydrogen bonds between MCB and UA.

**TABLE II**  
Glass-Transition Temperatures of the PB Block in SBS and Its Composites

	Composite			
	SBS	MCB/SBS (0.2 wt % MCB)	UA/SBS (2 wt % UA)	UA/MCB/ SBS (0.2 wt % MCB and 2 wt % UA)
Glass-transition temperature ( $^\circ\text{C}$ )	-87.4	-90.5	-89.7	-88.5

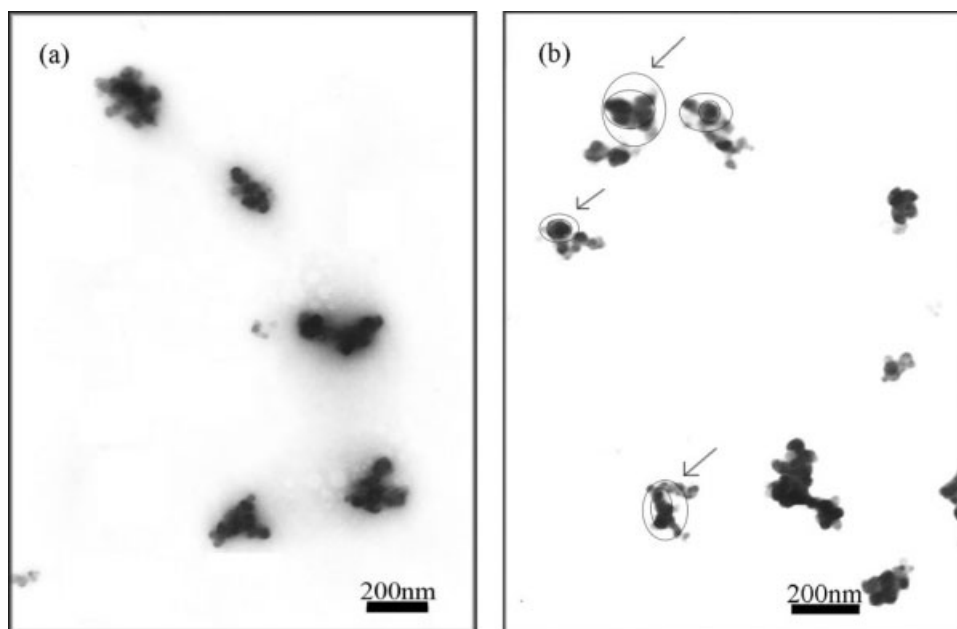


**Figure 10** TEM micrographs of the SBS composites: (a) 2 wt % UA/0.2 wt % CB/SBS and (b) 2 wt % UA/0.2 wt % MCB/SBS.

### CONCLUSIONS

Hydroxyl and hydroxymethyl groups were successfully introduced onto the surface of CB by oxidation and hydroxymethylation reactions, and the existence of these groups was proven by FTIR spectroscopy.

For the same polymer matrix, whether MCB or UA was used alone, a synergism effect for UV absorption did not occur. On the contrary, a distinct synergism arose when MCB and UA were combined in the same matrix, and the UV absorption was enhanced and ranged from 300 to 400 nm. The effective UV absorption range of the ternary composites was greatly extended and was about 25 nm compared with the corresponding binary composites. The synergism resulted from the interaction between UA and MCB, which mainly included hydrogen bonds formed between UA and MCB.

### References

- Lapidot, N.; Gans, O.; Biagini, F.; Sosonkin, L.; Rottman, C. *J Sol-Gel Sci Technol* 2003, 26, 67.
- Herzog, B.; Huglin, D.; Borsos, E.; Stehlin, A.; Luther, H. *Chimia* 2004, 58, 554.
- Introduction of Polymer Photochemistry; Wu, S. K., Ed.; Science Press: Beijing, 2003.
- Mahltig, B.; Bottcher, H.; Rauch, K.; Dieckmann, U.; Nitsche, R.; Fritz, T. *Thin Solid Films* 2005, 485, 108.
- Jager, C.; Henning, T. H.; Schlogl, R.; Spillecke, O. *J Non-Cryst Solids* 1999, 258, 161.
- Michel, B.; Henning, T. H.; Jager, C.; Kreibig, U. *Carbon* 1999, 37, 391.
- Liu, M.; Horrocks, A. R. *Polym Degrad Stab* 2002, 75, 485.
- Pena, J. M.; Allen, N. S.; Edge, M.; Liauw, C. M.; Valange, B. *Polym Degrad Stab* 2001, 72, 259.
- Horrocks, A. R.; Liu, M. *Macromol Symp* 2003, 22, 199.
- Liu, T. Q.; Portilla, R. C.; Belmont, J.; Matyjaszewski, K. *J Polym Sci Part A: Polym Chem* 2005, 43, 4695.
- Lin, Y.; Smith, T. W.; Alexandridis, P. *J Colloid Interface Sci* 2002, 255, 1.
- Yang, Q.; Wang, L.; Xiang, W. D.; Zhou, J. F.; Li, J. H. *Polymer* 2007, 48, 2866.
- Yang, Q.; Wang, L.; Xiang, W. D.; Zhou, J. F.; Jiang, G. H. *J Appl Polym Sci* 2007, 103, 2086.
- Borah, D.; Satokawa, S.; Kato, S. *Appl Surf Sci* 2008, 254, 3049.
- Li, Q. Y.; Yu, N.; Qiu, Z. X.; Zhou, X. J.; Wu, C. F. *Colloid Surf A* 2008, 317, 87.
- Fechine, G. J. M.; Rabello, M. S.; Souto-Maior, R. M. *Polym Degrad Stab* 2002, 75, 153.
- Wu, C. F.; Otani, Y.; Namiki, N.; Emi, H.; Nitta, K. H.; Kubota, S. *J Appl Polym Sci* 2001, 82, 1788.
- Sui, G.; Liang, J.; Zhu, Y. F.; Zhou, X. W. *High-Tech Commun* 2004, 14, 41.
- Hideto, T.; Yoshio, K.; Hirofumi, T.; Saburo, T. *Polymer* 2007, 48, 4213.